

Effects of functional groups at perylene diimide derivatives on organic photovoltaic device application

Won Suk Shin,^{*a} Hwan-Hee Jeong,^a Mi-Kyoung Kim,^a Sung-Ho Jin,^{*a} Mi-Ra Kim,^a Jin-Kook Lee,^b Jae Wook Lee^c and Yeong-Soon Gal^d

Received 13th September 2005, Accepted 1st November 2005

First published as an Advance Article on the web 16th November 2005

DOI: 10.1039/b512983d

Four soluble perylene diimide derivatives (**PDIs**) have been prepared and their UV-visible and photoluminescence (PL) spectroscopy, cyclic voltammetry (CV) and thermal properties were studied. ITO/PEDOT:PSS/poly(3-hexylthiophene) (**P3HT**):**PDIs**/LiF/Al photovoltaic devices were fabricated with **PDIs** as electron accepting and transporting materials. The highest incident photon-to-current conversion efficiency (IPCE) of 19% at 495 nm and the power conversion efficiency (PCE) of 0.18% under AM 1.5 (100 mW cm⁻²) with a short-circuit current density (J_{SC}) of 1.32 mA cm⁻², an open circuit voltage (V_{OC}) of 0.36 V, and a fill factor (FF) of 0.38 have been achieved with 1 : 4 ratio of **P3HT** : *N,N'*-di(1-nonadecyl)perylene-3,4,9,10-bis(dicarboximide) (**PDI-C9**) after annealing at 80 °C for 1 h. 1,7-Bis(*N*-pyrrolidinyl)-*N,N'*-dicyclohexyl-3,4,9,10-perylenebis(dicarboximide) (**5-PDI**), which has the electron donating pyrrolidinyl group, absorbed the long wavelength region to give IPCE onset higher than 750 nm and the pyrrolidinyl group also raised the LUMO level of **5-PDI** to render the high V_{OC} (up to 0.71 V) in photovoltaic device.

Introduction

Organic materials for photovoltaic devices based on conducting polymers are attractive because most of them can be processed from solution *via* spin-coating at room temperature, enabling the manufacture of large area, flexible and light-weight devices. Besides environmental constraints and the predictable exhaustion of fossil energy resources, the strong renewal of interest for organic photovoltaic conversion has been boosted by the large improvement in conversion efficiency of organic solar cells accomplished in recent years.¹ Current progress on organic photovoltaic devices from the standpoint of increasing power conversion efficiency (PCE) is mainly attributed to the bulk heterojunction structure, which enables an efficient charge separation due to the increased photoactive interface area of p-n junction. The bulk heterojunction is typically attained by blending a donor (p-type) conjugated polymer and an acceptor (n-type) molecule. The highest efficiency of 3.5% has been reported so far,^{1a} and recently 5% efficiency benchmark has been overcome.^{1b} But, further increase of the PCE is required for commercial applications of organic photovoltaic solar cells.² The search for new materials with good performance characteristics as well as the improvement in the device fabrication has been a subject of importance.

Organic photovoltaic devices rely on three main processes, namely, exciton generation, exciton dissociation, and free

charge collection. First, excitons are generated in the active layer by absorbing incident light, then excitons diffuse in the active layer and dissociate at the interface between the two materials with different electron affinities to form free charge carriers, and, finally, charge carriers are transported to the anode and the cathode, driven by a difference in chemical potential.³

As an energy-conversion device, efficiency is a very important parameter. In order to increase the PCE of devices, many aspects should be taken into account, such as the absorption coefficients of the materials, the exciton dissociation rates and the charge-carrier mobilities. First of all, the active layer should absorb as many as possible of the incident photons to generate excitons. The thickness of the active layer is, however, limited by the low carrier mobility of most organic materials, and is, typically, of the order of hundreds of nanometres.⁴ Most of the electron acceptors such as C₆₀ derivatives and TiO₂ nanoparticles for bulk heterojunction photovoltaic devices have relatively weak molar absorption coefficients at the visible region and do not give any direction for self-assembly while they were blended with electron donor polymers. We are interested in perylene diimide derivatives (**PDIs**), because **PDIs** have large molar absorption coefficients, good electron accepting properties⁵ and possible generation of a highly conducting direction along the π - π stacking axis,^{6,7} in addition to the other merits, like robust, thermally stable, and inexpensive. Up to date, most of the applications for photovoltaic devices with perylene derivatives were performed to dye-sensitized solar cell (DSSC)⁸ or layered structure through vapor deposition with insoluble **PDIs**,⁹ but applications of **PDIs** to the bulk heterojunction photovoltaic devices are quite limited.¹⁰

Thus, in this paper we have undertaken a systematic study on various **PDIs**, which have different functional groups, to

^aDepartment of Chemistry Education and Center for Plastic Information System, Pusan National University, Busan 609-735, Korea.

E-mail: shinws@pusan.ac.kr; shjin@pusan.ac.kr; Fax: +82 51 581 2348; Tel: +82 51 510 3524 Tel: +82 51 510 2727

^bDepartment of Polymer Science and Engineering, Pusan National University, Busan 609-735, Korea

^cDepartment of Chemistry, Dong-A University, Busan 604-714, Korea

^dPolymer Chemistry Lab., Kyungil University, Hayang 712-701, Korea

find the most promising acceptor structure for the future bulk heterojunction photovoltaic devices. We chose four different **PDI**s: *N,N'*-di(1-nonadecyl)perylene-3,4,9,10-bis(dicarboximide) (**PDI-C9**), 1,7-bis(*N*-pyrrolidinyl)-*N,N'*-dicyclohexyl-3,4,9,10-perylenebis(dicarboximide) (**5-PDI**), 2-(1-nonyldecyl)benzimidazo[2,1-*a*]anthra[2,1,9-*def*:6,5,10-*d'e'f'*]diisoquinoline-1,3,8(*2H*)-trione (**PDI-BI**), and *N,N'*-bis(cyclohexyl)-(1,7 & 1,6)-dicyanoperylene-3,4,9,10-bis(dicarboximide) (**PDI-CN**). **PDI-C9** has similar structure with *N,N'*-bis(1-ethylpropyl)-3,4,9,10-perylene bis(tetracarboxyl diimide) (**EP-PTC**)^{10a} of Friend's group, but has longer alkyl chains to give better solubility in solution and to have better miscibility with **P3HT** in solid state. We designed more planar **PDI-BI** to give better stacking property than **PDI-C9** while maintaining reasonable solubility with its swallow-tailed long alkyl chain. Introduction of pyrrolidyl group at the bay position of perylene shifted the absorption region to longer wavelength¹¹ and the absorption maximum of **5-PDI** was observed at 700 nm. **PDI-CN** has high charge mobility as an organic thin-film transistor (OTFT) material,¹² which is one of the most desired properties for bulk heterojunction photovoltaic device materials.

The conjugated polymer poly(3-hexylthiophene) (**P3HT**), which is known to be a good hole mobility molecule in its regioregular form,¹³ has been chosen as an electron donor as well as a hole conductor. Fixing **P3HT** as a hole transporting polymer and varying the electron acceptor **PDI**s, we can assume that the observed properties differences in devices are mainly come from the different structural and physical properties of **PDI**s. The compound structures are shown in Fig. 1.

Results and discussion

It was already demonstrated that increased ordering of perylene molecules leads to an increase in exciton diffusion

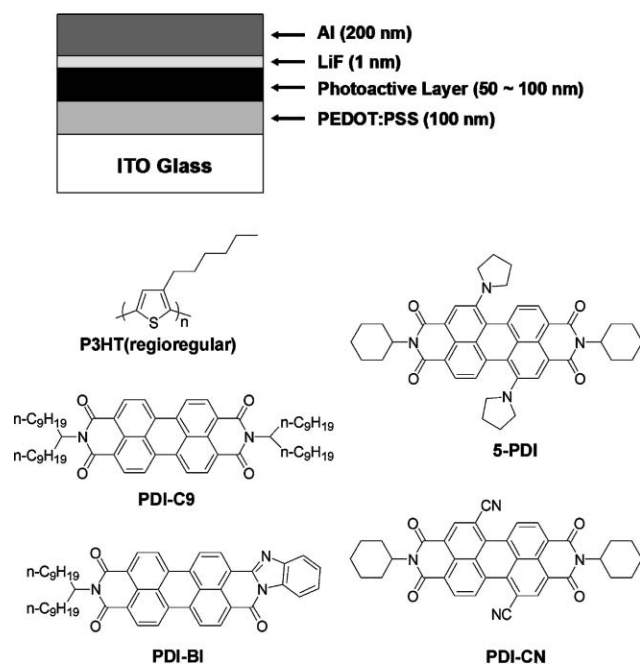


Fig. 1 Device configuration and the chemical structures of **P3HT** and perylene diimide derivatives (**PDI**s).

length¹⁷ and stabilizes the charge separated states, which slows down the charge recombination.¹⁸ UV-visible spectroscopic results of **PDI**s are presented in Fig. 2 and the optical properties are given in Table 1. From these results, it is evident that when **PDI**s cast from chloroform solution to solid state film, the full width at half maximum (FWHM) of **PDI-BI** and **PDI-CN** in solid films increase to become much broader than **PDI-C9** and **5-PDI**, which implies that the planar structures of **PDI-BI** and **PDI-CN** have a better stacked structure in solid state than **PDI-C9** and **5-PDI**. The maximum absorption peaks of all **PDI**s in solid film had a hypsochromic shift while they solidified during spin casting from chloroform solution. This blue shift was caused by the H-aggregation of perylene moiety, which means **PDI**s were aggregated *via face to face self-assembly*⁶ (Table 1 and Fig. 2). The extended H-aggregation in the donor polymer blended device could give the charge transporting channel along the π - π stacking axis.^{6,7} With long wavelength visible light absorption up to 800 nm in the film state, **5-PDI** could be a good candidate to use the whole range of visible light by fabricating photovoltaic device after mixing with **P3HT**, while the other **PDI**s did not effectively absorb light of longer wavelength than 670 nm.

PL quenching in donor-acceptor composites is a useful indication for the efficient charge transfer between the two

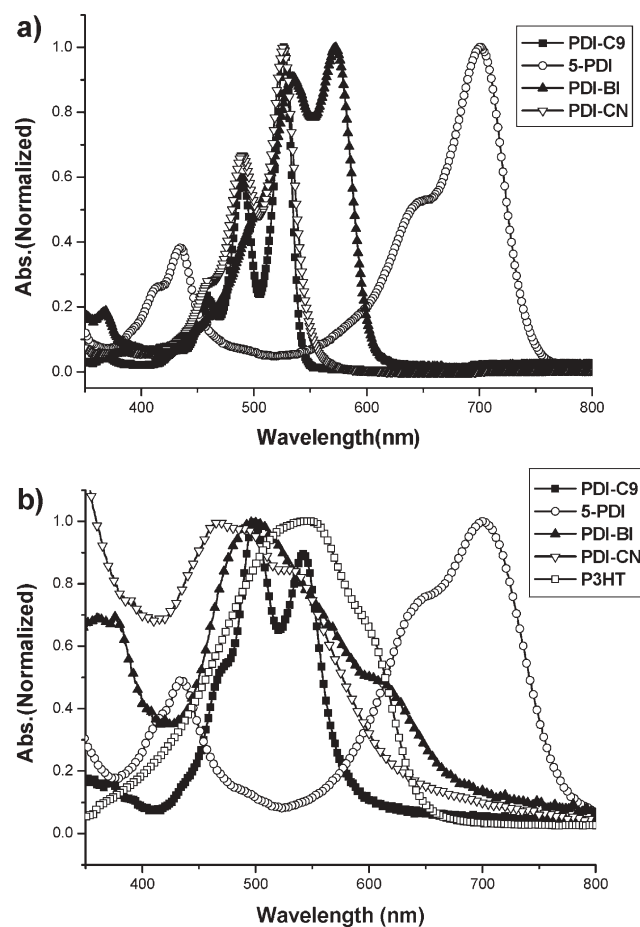


Fig. 2 UV-Visible spectra of (a) **PDI**s in chloroform solution, (b) thin films of **PDI**s and **P3HT** spin-coated on quartz from chloroform solution.

Table 1 Glass transition temperatures and the optical properties of PDIs

Compounds	PDI-C9	5-PDI	PDI-BI	PDI-CN
$T_g^a/^\circ\text{C}$	76 and 93	105	124	135
$\lambda_{\text{abs max}}$ in solution ^b /nm	527 (490 ^e)	701	572 (535 ^e)	526 (490 ^e)
FWHM ^c in solution ^b /nm	18 (50 ^f)	85	86	30 (52 ^f)
Φ_{PL} in solution ^b ($\lambda_{\text{ex}}/\lambda_{\text{PL,max}}$) [% (nm/nm)]	77 (500/534)	5.9 (680/726)	28 (550/597)	64 (490/535)
$\lambda_{\text{abs max}}$ in film ^d /nm	499 (542 ^e)	700	499	467
FWHM ^c in film ^d /nm	92	126	154	>200
Φ_{PL} (%) in film ^d ($\lambda_{\text{ex}}/\lambda_{\text{PL,max}}$) [% (nm/nm)]	52 (542/608)	— ^g	— ^g	0.09 (537/629)

^a Onset temperature. ^b Chloroform solution. ^c Full width at half maximum. ^d Spin cast on quartz plate from chloroform solution. ^e Second highest peak. ^f Assumed FWHM as if the 490 nm peak were merged to the 526–527 nm peak. ^g Not detected.

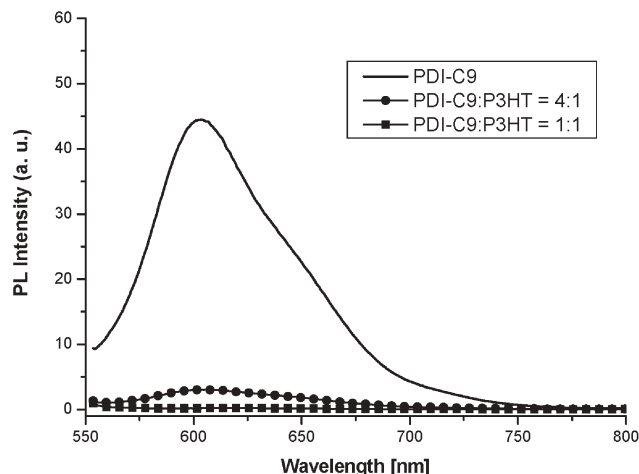


Fig. 3 PL spectra of the PDI-C9:P3HT blend films upon excitation at 542 nm. PDI-C9:P3HT blend films were spin-coated on quartz from chloroform solution.

components.^{10b,19} Only PDI-C9 shows good PL quantum efficiency in both the solution (77%) and film state (52%) (Table 1). In the film state all other PDIs do not have reasonable photoluminescence. Fig. 3 shows the PL spectra of the PDI-C9:P3HT composite films with different concentrations of P3HT. The results exhibit a significant PL quenching of the PDI-C9 emission in the composites. With more than 20% of the P3HT, most of the PL is quenched. This observation obviously indicates that the charge transfer from P3HT to PDI-C9 through the absorption of light by PDI-C9 and the back-transfer proceed with the nonradiative recombination process.²⁰ This result implies that the light, which is absorbed by the PDIs, also could contribute to the generation of current at the photovoltaic device.

Thermogravimetric analysis (TGA) data of PDIs revealed that all the PDIs are thermally stable over 400 °C except 5-PDI

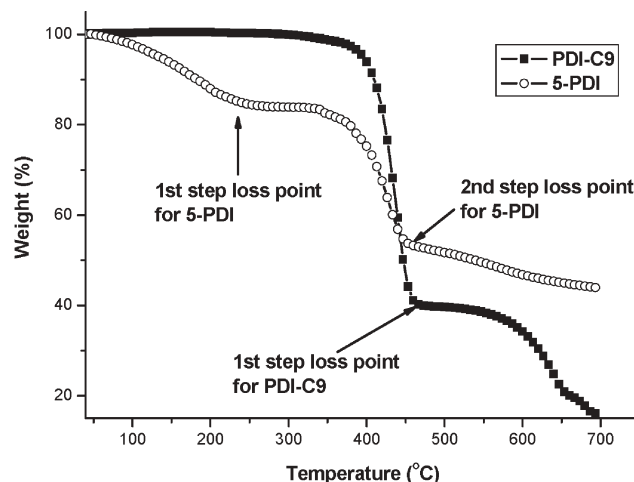


Fig. 4 Thermogravimetric analysis (TGA) graph of PDI-C9 and 5-PDI.

as given in Table 2. 5-PDI loses 16% of weight at 233 °C (first step loss point) and retained 80% of its weight at the end of the flat region (373 °C) as shown in Fig. 4, which is well matched with the calculated 20% weight loss by losing the pyrrolidiny group. By losing a cyclohexyl group, it additionally reduces the weight to 54% at the second step loss point (453 °C), theoretically 56% of 5-PDI's weight will be retained after losing both the pyrrolidiny and cyclohexyl group. Three of the other PDIs were stable up to 400 °C and lost the alkyl group at the diimide nitrogen (1-nonadecyl- or cyclohexyl-) near 460–513 °C at the first step loss point (Fig. 4 and Table 2).

From the TGA data, we can conclude that the benzimidazole group in PDI-BI and the nitrile group in PDI-CN are thermally stable and the alkyl groups at the diimide amine are also quite stable over 400 °C, but the amine group attached at the bay position of perylene was easily decomposed, even below 200 °C.

Table 2 Thermogravimetric analysis (TGA) of PDIs

Compounds	5% Weight loss temperature/°C	First step loss point, ^a weight at that point (losing functional group, calcd. weight after loss)	Second step loss point, ^a weight at that point (losing functional group, calcd. weight after loss)
PDI-C9	395	473 °C, 40% (1-nonadecyl, 42%)	—
5-PDI	133	233 °C, 84% (pyrrolidiny, 80%)	453 °C, 54% (cyclohexyl, 56%)
PDI-BI	408	513 °C, 67% (1-nonadecyl, 63%)	—
PDI-CN	413	460 °C, 77% (cyclohexyl, 73%)	—

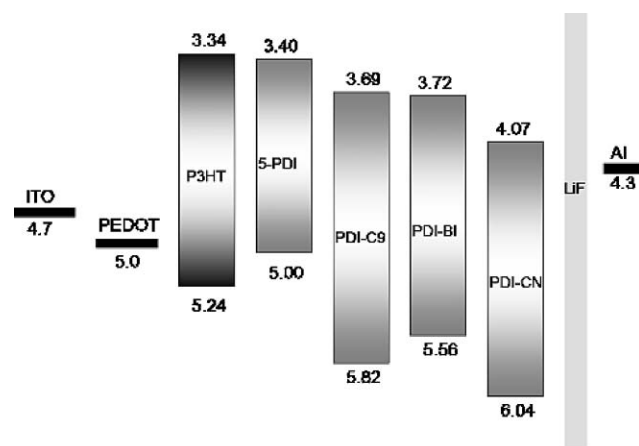
^a Stabilizing point after the 1st or 2nd step loss.

Table 3 Electrochemical properties and the estimated MO energies of the **PDIs** and **P3HT** with respect to the vacuum level

Compounds	$E_{1/2}^{+2}/V$	$E_{1/2}^{+1}/V$	$E_{1/2}^{-1}/V$	$E_{1/2}^{-2}/V$	$E_{1/2}^{-3}/V$	Optical band gap in film/eV	HOMO ^d	LUMO ^d
PDI-C9 ^a	—	—	-1.11	-1.37	—	2.13	5.82 ^e	3.69 ^e
5-PDI ^a	0.32	0.17	-1.40	-1.52	—	1.60	5.00 ^e	3.40 ^e
PDI-BI ^a	—	—	-1.08	-1.26	—	1.84	5.56 ^e	3.72 ^e
PDI-CN ^a	—	—	-0.73	-1.05	-1.53	1.97	6.04 ^e	4.07 ^e
P3HT ^b	—	0.57 ^c	—	—	—	1.90	5.24 ^f	3.34 ^f

^a Half way potential of all **PDIs** vs. Fc/Fc⁺ were determined in solution state with 0.1 M Bu₄NPF₆ in CH₂Cl₂ solution. ^b In solid state with 0.1 M Bu₄NBF₄ in CH₃CN solution. ^c Onset potential. ^d Set ferrocene-ferrocenium = 4.80 eV. ^e From $E_{1/2}^{-1}$ and optical band gap in film. ^f From onset potential and optical band gap in film.

Cyclic voltammetry (CV) is a useful method for measuring electrochemical behavior, evaluating the relative HOMO and LUMO energy levels and the band gap of a molecule. In order to calculate the absolute energies of HOMO and LUMO levels, the redox data are standardized with ferrocene-ferrocenium couple, which has a calculated absolute energy of -4.8 eV.²¹ The LUMO energy levels of **PDIs** were obtained from the half way reduction potentials ($E_{1/2}^{-1}$). However, the oxidation potentials of **PDI-C9**, **PDI-BI** and **PDI-CN** were not observed clearly in CV measurements, hence the HOMO levels of **PDIs** were estimated by the addition of the optical band gap from the LUMO levels. The HOMO energy level of the **P3HT** was obtained from the onset potential of the oxidation at CV, and the LUMO was estimated by the subtraction of the optical band gap from the HOMO level. The optical band gaps of all **PDIs** and **P3HT** were determined by the absorption edge of their thin films. The resulting hypothesized energy band gap and energy diagram can be seen in Table 3 and Fig. 5. **PDI-C9** and **PDI-BI** have the proper HOMO and LUMO levels to accept an electron from the excited **P3HT** molecule and to transfer the hole at the excited **PDIs** to **P3HT**. But for **5-PDI**, HOMO level was higher than the HOMO level of **P3HT** and it could have some possibility to render the undesired energy transfer from **P3HT** to **5-PDI** rather than charge separation. At the case of **PDI-CN**, both the HOMO and LUMO levels were too low. The LUMO level of the **PDI-CN** was close to the work function of Al, and it could reduce the built-in potential of device and possibly reduce the open circuit voltage (V_{OC}).

**Fig. 5** Hypothesized energy diagram of ITO/PEDOT:PSS/P3HT:PDIs/LiF/Al devices.

Photovoltaic measurements were performed using an AM 1.5 solar simulator and the intensity of the incident light was 100 mW cm⁻². The measurements were made at ambient atmosphere. The power conversion efficiency (PCE) of the solar cell device was calculated from the values of open-circuit voltage (V_{OC}) and short-circuit current density (J_{SC}) as the following equation:

$$PCE = P_{out}/P_{in} = (J_{SC} \times V_{OC}) \times FF/P_{in}$$

P_{in} represented the incident light power [mW cm⁻²]. And fill factor (FF) was calculated from the values of V_{OC} , J_{SC} , and the maximum power point (P_{max}), as the following equation:

$$FF = P_{max}/(J_{sc} \times V_{oc}) = (J_{max} \times V_{max})/(J_{sc} \times V_{oc})$$

where J_{max} and V_{max} is maximum current density and maximum voltage at the P_{max} , respectively. Table 4 summarizes photovoltaic device performance results for ITO/PEDOT:PSS/P3HT:PDIs/LiF/Al devices. First, we fabricated the devices with 1 : 1 ratio of **P3HT** : **PDIs** as an active layer without annealing (**device b, d, j, l, p** and **s** in Table 4). Among these devices, **PDI-BI** showed the best PCE of 0.061% (**device p**); this higher efficiency over **PDI-C9** was caused by its wider absorption band and better stacking ability by the planar structure than **PDI-C9**. Annealing of the **PDI-C9** devices at 80 °C for 1 h under Ar atmosphere drastically increased the PCE nearly twofold (**device a** and **e**), while the other **PDIs** devices did not show any meaningful differences (**device i, k, o, q** and **r**). The increased device performance in the case of **PDI-C9** devices may be due to the reorientation of **P3HT**¹⁰ and **PDI-C9** to get more ordered stacking during annealing. Low T_g of **PDI-C9** ($T_g = 76$ °C at Table 1) can cause the possible reorientation of **P3HT** and the high T_g of the other **PDIs** (T_g of **5-PDI** = 105 °C, T_g of **PDI-BI** = 124 °C and T_g of **PDI-CN** = 135 °C) prevent the formation of the more ordered structure of these at this low annealing temperature. **PDI-CN** showed the good electron transporting properties upon vapor deposition on OTFT device,¹² but the solution cast device with **P3HT** has poor short-circuit current density (J_{SC}). This may be due to the poor morphology of the spin cast film because of its poor solubility and the too good aggregating ability of **PDI-CN**.

With increasing **PDI-C9** ratio in **P3HT**:**PDI-C9** blending system, the PCE also increased and reached to a maximum of 0.18%, when the device was annealed at 80 °C for 1 h (**device g** in Table 4). However, in case of **5-PDI** based device, the decrease in PCE was observed with increasing the blending ratio (**device g-n**). This reduction in PCE may be due to the presence of two pyrrolidinyl groups in **5-PDI**, which inhibits

Table 4 Performance of ITO/PEDOT:PSS/P3HT:PDIs/LiF/Al bulk heterojunction photovoltaic devices under a simulated photovoltaic light with 100 mW cm⁻² illumination (AM1.5)

Compounds	Device	P3HT/PDI ratio	Active layer thickness/nm	Annealing ^a	$J_{SC}/\text{mA cm}^{-2}$	V_{OC}/V	FF	PCE [%]
PDI-C9	a	1/1	100	Yes	0.45	0.26	0.31	0.036
	b	1/1	100	No	0.30	0.19	0.32	0.018
	c	1/1	70	Yes	0.67	0.29	0.33	0.065
	d	1/1	70	No	0.47	0.23	0.31	0.034
	e	1/2	100	No	0.55	0.30	0.31	0.051
	f	1/2	70	No	0.73	0.27	0.35	0.068
	g	1/4	70	Yes	1.32	0.36	0.38	0.182
	h	1/4	70	No	1.31	0.30	0.38	0.139
5-PDI	i	1/1	100	Yes	0.26	0.66	0.25	0.043
	j	1/1	100	No	0.25	0.63	0.27	0.043
	k	1/1	70	Yes	0.27	0.51	0.30	0.041
	l	1/1	70	No	0.28	0.55	0.27	0.042
	m	1/2	90	No	0.20	0.61	0.30	0.037
	n	1/4	70	No	0.21	0.71	0.21	0.031
	o	1/1	85	Yes	0.40	0.38	0.29	0.044
PDI-BI	p	1/1	70	No	0.47	0.37	0.35	0.061
	q	1/1	80	Yes	0.04	0.13	0.29	0.002
PDI-CN	r	1/1	50	Yes	0.13	0.13	0.30	0.005
	s	1/1	50	No	0.12	0.12	0.30	0.004

^a 80 °C for 1 h under Ar atmosphere.

the well stacking of **5-PDI** itself. Apart from this, the good solubility of **5-PDI** and also the good miscibility with **P3HT** inhibits the ordered structure of **P3HT**, which resulted in the limited charge transporting ability in **P3HT**. The representative current potential characteristics with different functional groups are presented in Fig. 6.

The incident photon-to-current conversion efficiency (IPCE) can be obtained from the short-circuit current density (J_{SC}) upon monochromatic illumination in the 380–750 nm region:

$$\text{IPCE} = \frac{\text{\#electrons}}{\text{\#photons}} = 1240 \times \frac{J_{SC}}{P_{in}\lambda}$$

Where J_{SC} is the short-circuit current density [mA cm^{-2}], P_{in} the incident light power [mW cm^{-2}], and λ the wavelength [nm]. The

IPCE spectra closely follow the UV–visible absorption spectra of **P3HT:PDIs** blending films (Fig. 7). The IPCE of the device made with **PDI-C9** (device **g**) reached a maximum of 19% at 495 nm but light with a longer wavelength than 670 nm did not generate any photocurrent (Fig. 7(a)), which is well matched with the UV–visible spectrum of **PDI-C9 : P3HT = 1 : 4** film. In the case of device **j**, the IPCE spectrum was also similar to absorption spectrum of **P3HT : 5-PDI = 1 : 1** blending film, which covered the whole visible region. And the onset of IPCE spectrum was at a longer wavelength than 750 nm (Fig. 7(b)) meaning the light absorbed by **5-PDI** generates the photocurrent. From previous PL quenching results and these IPCE experiments, we could say that the light absorbing electron transporting materials, **PDIs**, also contribute the harvesting of sunlight.

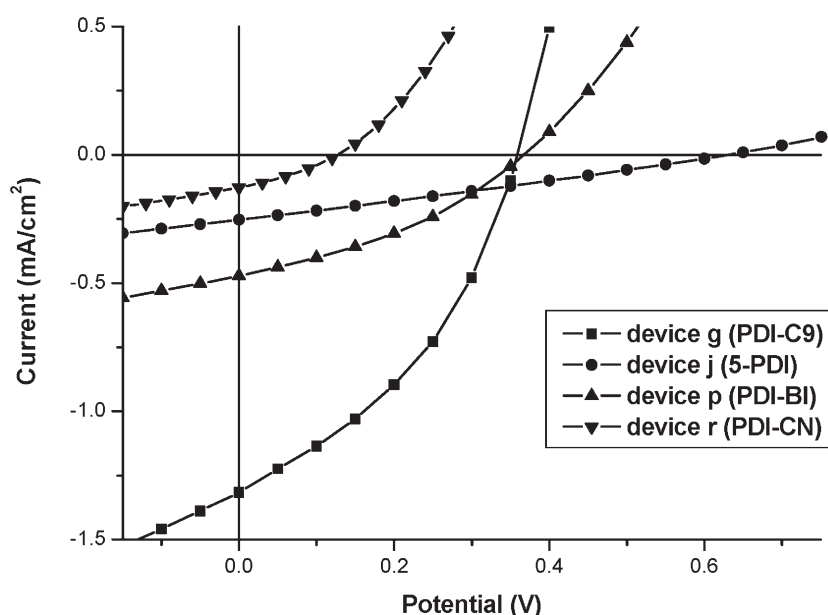


Fig. 6 Representative current potential characteristics for ITO/PEDOT:PSS/P3HT:PDIs/LiF/Al devices. Detailed data of each graph could be found in Table 4.

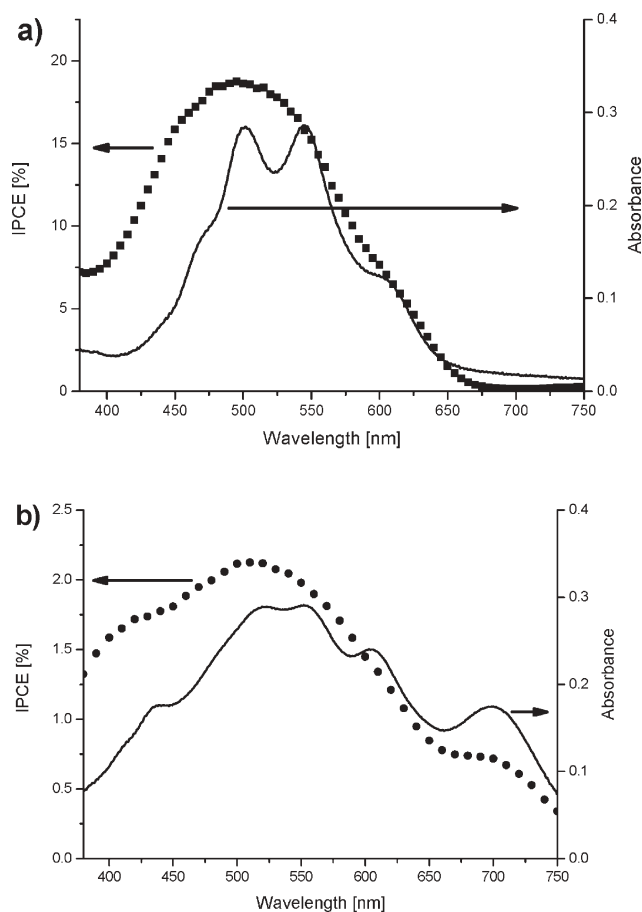


Fig. 7 UV-visible absorption spectra of **P3HT:PDI**s blend films and incident photon-to-current conversion efficiency (IPCE) spectra of devices: (a) **P3HT : PDI-C9 = 1 : 4** (device **g** at Table 4); (b) **P3HT : 5-PDI = 1 : 1** (device **j** in Table 4). **P3HT:PDI**s blend films were spin-coated on quartz from chloroform solution.

From the above results, we can conclude some important information regarding the architecture of perylene molecules. **PDI-C9** has a good solubility to apply solution processed photovoltaic device fabrication because of its long swallow tailed alkyl chains and shows the best photovoltaic properties among the four **PDI**s, however the low open circuit voltage ($V_{OC} = \sim 0.36$ V) and short-circuit current density ($J_{SC} = 1.32$ mA cm⁻²) are its drawbacks. So, further structural modification is required to increase the V_{OC} and improve the electron transporting ability. When an electron donating group is fixed with **P3HT**, the V_{OC} is attributed to the LUMO level of the **PDI**s, so the introduction of electron donating group at the perylene body could increase the V_{OC} by increasing LUMO level. Actually the increase of LUMO level by 0.3 V with introducing electron donating pyrrolidinyl group renders the increase of V_{OC} nearly 0.3 V at **5-PDI** ($V_{OC} = \sim 0.6$ V). This is quite well matched with the variation of the valence band of n-type semiconductor results in a change of the open circuit voltage with a scaling factor of ~ 1 .^{1b} However, pyrrolidinyl groups interfere with the construction of the ordered structure to become a better electron transporting channel, also rendering the poor thermal stability to **5-PDI** as shown at the TGA data. One way to improve the electron

transporting ability of the perylene acceptors was the introduction of more flat structure like **PDI-BI** and **PDI-CN**, but these acceptor molecules have higher T_g than annealing temperature (80 °C), hence the device efficiency could not be improved by reorientation of donor-acceptor molecules through annealing. The worst case is the **PDI-CN**: we only could fabricate the device after filtering out insoluble **PDI-CN** parts because of its poor solubility.

To design ideal perylene, thermally stable electron donating substituent would be a prerequisite, because this electron donating group will improve the V_{OC} by increasing LUMO level of perylene and possibly shifts the absorbing region to the longer wavelength, but at the same time it should not restrict the self-assembly of perylene in order to maintain the electron transporting channel. The synthesized perylenes should also have proper T_g values, because too high T_g value of perylene molecules will restrict the reorientation of **P3HT** and perylene itself during annealing.

Conclusions

Different structural electron acceptor perylene derivatives were synthesized and characterized using UV-visible and photoluminescence (PL) spectroscopy, cyclic voltammetry, TGA, and DSC. The synthesized perylene derivatives were used as an electron acceptor molecule in the photovoltaic device fabrication along with **P3HT** as a donor molecule. The device fabricated using **PDI-C9** has shown better PCE when compared with other devices fabricated using other perylene molecules. Further, the PCE has increased to two-fold when the **PDI-C9** device was annealed at 80 °C for 1 h. However, the device with **P3HT:5-PDI** has absorbed the long wavelength region of light (>750 nm) and also raised the V_{OC} of the device.

Experimental

¹H NMR spectra were recorded in CDCl₃ on a Varian Mercury 300, and chemical shifts were recorded in ppm. The absorption and photoluminescence (PL) spectra were measured using a Jasco V-570 UV-vis spectrometer and a Hitachi F-4500 fluorescence spectrophotometer, respectively. The PL quantum yields of **PDI**s in chloroform solution were determined against 9,10-diphenylanthracene in ethanol as a standard ($\Phi_{PL} = 91\%$)¹⁴ and that of solid film state **PDI**s were estimated by using a thin film of $\sim 10^{-3}$ M 9,10-diphenylanthracene in poly(methyl methacrylate) as a standard ($\Phi_{PL} = 83\%$).¹⁵ Thermal analyses were carried out on a Mettler Toledo TGA/SDTA 851^e and DSC 822^e analyzer under N₂ atmosphere at a heating rate of 10 °C min⁻¹.

Synthesis and preparation of materials

Regioregular **P3HT** purchased from Aldrich and the poly(ethylenedioxythiophene) doped with poly(styrenesulfonic acid) (PEDOT:PSS, Baytron[®] PH) purchased from Baytron were used without further purification. 3,4,9,10-Perylene-tetracarboxylic dianhydride was supplied by Phthalos (South Korea). The **PDI-C9**,¹⁶ **5-PDI**¹¹ and **PDI-CN**¹² were synthesized and purified by literature methods. **PDI-BI** can be synthesized with the following procedure from

N-(1-nonadecyl)-3,4,9,10-perylenetetracarboxylic acid 3,4-anhydride-9,10-imide, which could be prepared from the selective hydrolysis of **PDI-C9**.¹⁶

Synthesis of 2-(1-nonyldecyl)-benzimidazo[2,1-*a*]anthra[2,1,9-*def*:6,5,10-*d'**e'**f'*]diisoquinoline-1,3,8(2*H*)-trione (**PDI-BI**)

N-(1-Nonadecyl)-3,4,9,10-perylenetetracarboxylic acid 3,4-anhydride-9,10-imide (0.30 g, 0.455 mmol), 1,2-phenylenediamine (0.054 g, 0.501 mmol) and imidazole (1.0 g) were dissolved in 50 ml of pyridine and then refluxed for 20 h under nitrogen atmosphere. The reaction mixture was cooled to room temperature and the solvent removed on a rotary evaporator. The resulting solid was chromatographed on silica using 95% chloroform–5% methanol as the eluent to get the product. The product was further purified by recrystallizing twice from hexane–chloroform to yield pure **PDI-BI** (0.20 g, 60%). ¹H NMR (CDCl₃): δ 8.10–8.45 (m, 8H), 7.82 (d, 1H), 7.38 (d, 1H), 7.05 (q, 2H), 5.18 (1H), 2.25 (2H), 1.92 (2H), 1.15 (28H), 0.91 (6H). HR-Mass (FAB⁺): 730.4011 (calcd. 730.4009 for (M + H)⁺).

Photovoltaic device fabrication

Films of different weight ratios of the **P3HT** and **PDIs** were spin coated from *o*-dichlorobenzene solution onto indium tin oxide (ITO) covered glass substrates that had been previously coated with 100 nm of PEDOT:PSS. Then, LiF (1 nm) and Al top electrode (200 nm) were deposited by means of thermal evaporation *in vacuo* (base pressure < 2.0 × 10⁻⁶ Torr) onto the organic layer through a shadow mask. The pixel size as defined by the overlap with ITO and Al back electrode was 4 mm². Thermal treatment was performed at 80 °C for 1 h under dry Ar atmosphere on a high precision hot stage. All other device fabrication steps and all the measurements were performed at ambient atmosphere. The current–voltage curve of the photovoltaic device was measured under the illumination of a simulated solar light with 100 mW cm⁻² (AM1.5) by an Orel 300W solar simulator. Electric data were taken using a Keithley 236 source-measure unit. Current–voltage responses were measured in the dark and under illumination. The photocurrent action spectra were carried out by illuminating the samples with a 300 W Xenon lamp, dispersed by Dongwoo-optron (South Korea) DM151i single-grating monochromator. Film thickness was measured using a KLA Tencor Alpha-step IQ surface profilometer.

Cyclic voltammetry (CV) measurements

CV experiments were performed with a computer controlled Bioanalytical Systems CV-50W voltametric analyzer. A Pt disk (diameter = 2 mm) was used as a working electrode along with a Pt wire as a counter, and Ag/AgNO₃ was used as a reference electrode. For the measurements, **PDIs** were dissolved in freshly distilled dichloromethane containing 0.1 M tetrabutylammonium hexafluorophosphate (Bu₄NPF₆) as a supporting electrolyte, while **P3HT** film was coated on platinum disk from chlorobenzene solution before measuring in 0.1 M tetrabutylammonium tetrafluoroborate (Bu₄NBF₄) containing acetonitrile. Bu₄NPF₆ and Bu₄NBF₄ were recrystallized twice

from ethanol and ethyl acetate respectively, then dried under vacuum prior to use. Other chemicals and acetonitrile (Aldrich, >99.8%, anhydrous, sealed under N₂ gas) were used as received.

Acknowledgements

This work was supported by the Ministry of Information & Communications, Korea, under the Information Technology Research Center (ITRC) Support Program. Authors also thank Dr. B. Vijaya Kumar Naidu for the kind discussion.

References

- (a) F. Padinger, R. S. Rittberger and N. S. Sariciftci, *Adv. Funct. Mater.*, 2003, **13**, 85; (b) C. J. Brabec, *Sol. Energy Mater. Sol. Cells*, 2004, **83**, 273; (c) H. Spanggaard and F. C. Krebs, *Sol. Energy Mater. Sol. Cells*, 2004, **83**, 125; (d) G. Hughes and M. R. Bryce, *J. Mater. Chem.*, 2005, **15**, 94.
- R. D. McConnell, *Renewable Sustainable Energy Rev.*, 2002, **6**, 273.
- C. J. Brabec, N. S. Sariciftci and J. C. Hummelen, *Adv. Funct. Mater.*, 2001, **11**, 15.
- (a) S. E. Shaheen, C. J. Brabec, N. S. Sariciftci, F. Padinger, T. Fromherz and J. C. Hummelen, *Appl. Phys. Lett.*, 2001, **78**, 841; (b) F. Zhang, E. Perzon, X. Wang, W. Mammon, M. R. Andersson and O. Inganäs, *Adv. Funct. Mater.*, 2005, **15**, 745.
- E. E. Neuteboom, S. C. J. Meskers, P. A. Van Hal, J. K. J. Van Duren, E. W. Meijer, R. A. J. Janssen, H. Dupin, G. Pourtois, J. Cornil, R. Lazzaroni, J.-L. Bredas and D. Beljonne, *J. Am. Chem. Soc.*, 2003, **125**, 8625.
- T. Boom, R. T. Hayes, Y. Zhao, P. J. Bushard, E. A. Weiss and M. R. Wasielewski, *J. Am. Chem. Soc.*, 2002, **124**, 9582.
- S.-G. Liu, G. Sui, R. A. Cormier, R. M. Leblanc and B. A. Gregg, *J. Phys. Chem. B*, 2002, **106**, 1307.
- (a) S. Ferrere and B. A. Gregg, *New J. Chem.*, 2002, **26**, 1155; (b) S. Wang, Y. Li, C. Du, Z. Shi, S. Xiao, D. Zhu, E. Gao and S. Cai, *Synth. Met.*, 2002, **128**, 299.
- (a) J. Nakamura, C. Yokoe, K. Mruata and K. Takahashi, *J. Appl. Phys.*, 2004, **96**, 6878; (b) R. Bettignies, Y. Nicolas, P. Blanchard, E. Levillain, J.-M. Nunzi and J. Roncali, *Adv. Mater.*, 2003, **15**, 1939; (c) A. J. Breeze, A. Salomon, D. S. Ginley, B. A. Gregg, T. Tillmann and H.-H. Horhold, *Appl. Phys. Lett.*, 2002, **81**, 3085; (d) J. Y. Kim and A. J. Bard, *Chem. Phys. Lett.*, 2004, **383**, 11.
- (a) J. J. Dittmer, E. A. Marsaglia and R. H. Friend, *Adv. Mater.*, 2000, **12**, 1270; (b) E. E. Neuteboom, S. C. J. Meskers, P. A. Van Hal, J. K. J. Van Duren, E. W. Meijer, R. A. J. Janssen, H. Dupin, G. Pourtois, J. Cornil, R. Lazzaroni, J.-L. Bredas and D. Beljonne, *J. Am. Chem. Soc.*, 2003, **125**, 8625; (c) Y. Liu, C. Yang, Y. Li, Y. Li, S. Wang, J. Zhuang, H. Liu, N. Wang, X. He, Y. Li and D. Zhu, *Macromolecules*, 2005, **38**, 716.
- Y. Zhao and M. R. Wasielewski, *Tetrahedron Lett.*, 1999, **40**, 7047.
- B. A. Jones, M. J. Ahrens, M.-H. Yoon, A. Facchetti, T. J. Marks and M. R. Wasielewski, *Angew. Chem., Int. Ed.*, 2004, **43**, 6363.
- (a) Z. Bao, A. Dodabalapur and A. J. Lovinger, *Appl. Phys. Lett.*, 1996, **69**, 4108; (b) H. Sirringhaus, N. Tessler and R. H. Friend, *Science*, 1998, **280**, 1741.
- H. S. Joshi, R. Jamshidi and Y. Tor, *Angew. Chem., Int. Ed.*, 1999, **38**, 2722.
- X. Zhang, A. S. Shetty and S. A. Jenekhe, *Macromolecules*, 1999, **32**, 7422.
- L. D. Wescott and D. L. Mattern, *J. Org. Chem.*, 2003, **68**, 10058.
- B. A. Gregg, *J. Phys. Chem.*, 1996, **100**, 852.
- P. M. Kazmaier and R. Hoffmann, *J. Am. Chem. Soc.*, 1994, **116**, 9684.
- N. S. Sariciftci, L. Smilowitz, A. J. Heeger and F. Wudl, *Science*, 1992, **258**, 1474.
- G. Yu, C. Zhang and A. J. Heeger, *Appl. Phys. Lett.*, 1994, **64**, 1540.
- J. Pommerehne, H. Vestweber, W. Guss, R. F. Mahrt, H. Bässler, M. Porsch and J. Daub, *Adv. Mater.*, 1995, **7**, 551.